Calculating a Free-Free Absorption Model for PKS 1718-649

Chris Williams
Student 1607421
HET 606

160742@swin.edu.au

Abstract

This paper discusses free-free absorption as the driver of spectral shape in gigahertz peaked spectrum (GPS) sources. Two models (Tingay and Murphy 2001; Bicknell et al. 1997) are applied to high-precision spectral data for the PKS 1718-649 GPS source gathered using the Australia Telescope Compact Array (ATCA) (Tingay and de Kool 2002). The suitability of each model is assessed against the ATCA data. The Bicknell et al. model provides an excellent fit and is tested against third party data at higher and lower frequencies to test its validity outside the range of the ATCA data. Outside the ATCA range the model is less accurate, and reasons are discussed.

1. Introduction

1.1. PKS 1718-649

The PKS 1718-649 radio source is associated with the galaxy NGC 6328. Galactic recession at 4105 km s^{-1} ($z = 0.0014$) (Fosbury et al. 1977) gives a distance of distance 56 Mpc assuming $H_0 = 75$ km s^{-1} Mpc^{-1} and makes PKS 1718-649 the closest GPS source (Tingay et al. 1997). Observations using the Southern Hemisphere VLBI Experiment (SHEVE, (Preston et al. 1989, and others)) revealed the structure of the source as two elements with a 6.8 mas separation, differing flux densities and spectral indices (Tingay et al. 1997).

1.2. Gigahertz Peaked Spectrum Sources

The unified theory of active galactic nuclei (AGN) posits an accretion disc surrounding a central black hole as the driver of radio emissions from these galaxies. The AGN radio emission spectrum, a steady power-law decline with frequency and no general maxima, is characteristic of non-thermal origins. Synchrotron emission from charged particles moving in strong magnetic fields is the most likely source. Such radiation is usually polarised as a result of the magnetic field. A combination of high and low speed obscuring clouds and viewing angle successfully explains the majority of AGN types and temporal variations within single AGN sources.

However, a class of AGN with a marked spectral peak in the 0.1 to 10 GHz range is not easily reconciled with a direct viewing of a synchrotron source. These sources, called gigahertz peaked spectrum (GPS) sources, display a steeply rising low-frequency flux density profile leading to the peak, followed by a high-frequency declining profile more akin to theoretical synchrotron sources. GPS sources typically display the following features (Bicknell et al. 1997):

- Compact (0.1-10 kpc) symmetric radio lobes.
- Steeply rising ($\langle\alpha\rangle \simeq -1$) low frequency spectra.
- Very powerful radio emission.
- Inverse relationship between source size and turnover frequency.
- Low source polarisation (1-3%).
- Disturbed isophotes in parent galaxies.
- Very luminous "narrow line" emission.
- Tight correlation between line luminosity and total radio power.

2. GPS Models

The absence of low frequency emission from GPS sources is generally modelled as absorption superimposed upon a synchrotron source. The absorption could reasonably come from synchrotron-self absorption (SSA), in which emissions are later absorbed by other particles in the plasma, from free-free absorption (FFA) in a plasma external to the source, or from induced Compton scattering (Kuncic et al. 1998). O'Dea (1998) notes that both SSA and FFA are consistent with GPS source observations but that Occam's razor would favour SSA.

This analysis concentrates on free-free absorption as the mechanism responsible for the peak flux density in the gigahertz region. FFA is a scattering process in which a photon impinges on a free electron, imparts energy, and changes the electron's trajectory. The electron must be in the vicinity of a positive ion in order for energy and momentum to be conserved, otherwise the electron cannot absorb.

2.1. Free-free Absorption Models

The FFA model assumes a synchrotron source with an intrinsic flux density profile:

$$B_{int}(\nu) = A\nu^{\alpha}$$

where frequency, ν, is in units of gigahertz. A typical AGN spectrum has $-1.3 \lesssim \alpha \lesssim -0.5$.

Tingay and Murphy (2001) utilise a model for FFA in which the intrinsic spectrum is modified by the presence of an idealised free-free absorbing plasma of optical depth, $\tau_{ff}(\nu)$, such that the observed flux density profile becomes:

$$B_{obs}(\nu) = A\nu^{\alpha}e^{-\tau_{ff}(\nu)}$$

The optical depth is a combination of many factors: frequency; plasma path length; temperature; number density of charged particles; and a Gaunt factor appropriate to the frequency, temperature, and mass of the particles concerned. An acceptable approximation of the radio frequency behaviour for an assumed hydrogen plasma with an estimated Gaunt factor allows the equation to be rewritten in the form:

$$B_{obs}(\nu) = A\nu^{\alpha}e^{-\tau_1\nu^{-2.1}} \tag{1}$$

where τ_1 is the free-free absorption coefficient at 1 GHz.

Bicknell et al. (1997), in attempting to provide a unified model for GPS and compact steep-spectrum (CSS) sources, derived a more complex model based on the physics of a relativistic jet smothered by an irregular, high density envelope of gas. Rather than assuming uniformity, the optical depth of the absorbing clouds, a, is assumed to vary between 0 and a maximum, a_0, according to a power-law distribution ($\propto a^p$). The power-law index, p, is greater than -1 and assumed to be close to 0. Substituting the power-law optical depth into the equation for absorption by a simple screen (Eq. 2) allowed the average value of I_ν to be derived (Eq. 3):

$$\begin{aligned} I_\nu &= A_\nu^{-\alpha}e^{-a\nu^{-2.1}} && (2) \\ \langle I_\nu \rangle &= A\frac{p+1}{a_0^p}\int_0^{a_0} e^{-a\nu^{-2.1}} a^p da \end{aligned}$$

$$
\begin{aligned}
&= A(p+1)\left(\frac{\nu}{\nu_0}\right)^{2.1(p+1)-\alpha}\int_0^{(\nu/\nu_0)^{-2.1}} u^p e^{-u} du \\
&= A(p+1)\left(\frac{\nu}{\nu_0}\right)^{2.1(p+1)-\alpha}\gamma\left[p+1, \left(\frac{\nu}{\nu_0}\right)^{-2.1}\right] \qquad (3)
\end{aligned}
$$

where $a_0 = \nu_0^{2.1}$ and ν_0 is the characteristic frequency and A includes a ν_0^{α} factor. Note the use of opposite sign convention to Tingay and Murphy for α. Bicknell et al. took equation 3 as a sufficiently accurate representation of the power spectrum after assuming that the parameter a_0 was not strongly variable over the emitting area. Bicknell et al. successfully applied this model to three different sources taken from earlier surveys. This model will be referred to as the BDO model.

3. Data Reduction

Data for this analysis, from Tingay and de Kool (2002), consists of 38 high-precision flux density observations between 1.4 and 9.2 GHz taken using the Australia Telescope Compact Array (ATCA). The observations fall into the four bands supported by the ATCA, with the majority of data from the 6 and 3 cm bands. Error bounds on the flux density measurements are typically < 0.010 Jy. The data are presented in table 1.

An implementation of the nonlinear least-squares (NLLS) Marquardt-Levenberg algorithm, in gnuplot, was used to fit equations 1 and 3 to the data. The algorithm makes use of error bounds to weight individual datum points during calculations but, given the degree of uniformity in tolerances, this is not expected to have a significant impact on the fit. The iterative fitting process stops when the change in weighted sum of the squared residuals (WSSR) between iterations falls below a set threshold. For these fits the WSSR threshold was set to $\Delta_{WSSR} < 10^{-9}$. In the case of the Bicknell et al. model, several fitting runs with varied starting parameters were required to converge on an acceptable fit because of several regions in parameter-space where the WSSR plateaued. The resulting fits are depicted in figure 1 and the fit coefficients in table 2.

For the BDO model the low frequency spectral index is $\alpha = -0.4$ (Bicknell et al. 1997, Eq. 5.8) and the high frequency index is $\alpha = 0.605$. The Tingay and Murphy model has a high frequency index $\alpha = -0.43$, a slightly lesser slope.

Table 1. ATCA high precision radio spectrum PKS 1718-649

ν (GHz)	Flux (Jy)	ν (GHz)	Flux (Jy)	ν (GHz)	Flux (Jy)
1.384	3.915 ± 0.007	5.296	4.799 ± 0.003	6.600	4.440 ± 0.006
1.680	4.202 ± 0.017	5.400	4.772 ± 0.003	6.704	4.411 ± 0.014
1.760	4.294 ± 0.005	5.504	4.749 ± 0.003	8.096	4.085 ± 0.003
2.496	4.847 ± 0.012	5.600	4.729 ± 0.005	8.200	4.065 ± 0.003
2.540	4.876 ± 0.011	5.704	4.697 ± 0.004	8.296	4.041 ± 0.007
4.496	4.983 ± 0.005	5.800	4.670 ± 0.004	8.400	4.025 ± 0.008
4.600	4.964 ± 0.005	5.904	4.639 ± 0.004	8.496	3.989 ± 0.006
4.696	4.939 ± 0.002	6.000	4.613 ± 0.004	8.600	3.970 ± 0.006
4.800	4.924 ± 0.004	6.104	4.591 ± 0.004	8.896	3.893 ± 0.004
4.896	4.902 ± 0.002	6.200	4.557 ± 0.004	9.000	3.874 ± 0.005
5.000	4.873 ± 0.002	6.304	4.528 ± 0.004	9.096	3.871 ± 0.005
5.096	4.854 ± 0.003	6.400	4.505 ± 0.004	9.200	3.840 ± 0.005
5.200	4.822 ± 0.003	6.504	4.471 ± 0.005		

Table 2. FFA model fit coefficients

Tingay & Murphy		Bicknell et al.	
A	10.44 ± 0.3	A	12.50 ± 0.03
α	-0.43 ± 0.02	α	0.605 ± 0.004
τ_1	1.92 ± 0.08	ν_0	4.01 ± 0.04
		p	-0.52 ± 0.002
RMS of residuals	18.8	RMS of residuals	1.3

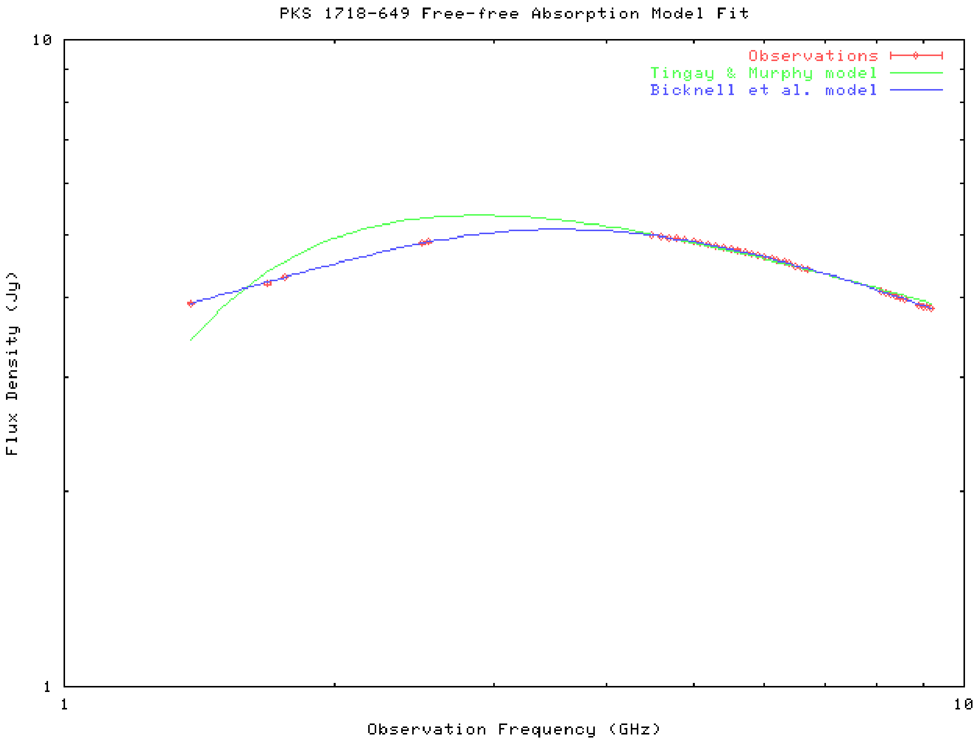

Fig. 1.— Data and plot of best fits for Tingay and Murphy, and BDO. models.

4. Results and Discussion

The Tingay and Murphy model fits reasonably well for frequencies above ≈ 4.5 GHz. In the high frequency range, the $\nu^{-2.1}$ term in equation 1 approaches 0 reducing the absorption term to unity, leaving an essentially unaltered synchrotron spectrum. Clearly the model does not fit the data well at the lower end of the frequency range, and this is reflected in the high residual figure. The peak indicated by this model is substantially stronger and lower in frequency than a visual approximation would indicate is reasonable for the data presented. Further, the low frequency roll-off is substantially steeper than the data would indicate. The basic assumption of this model is a uniform absorbing screen. The data would indicate that the absorption is more complex in nature than the model. This model will not be tested further.

The BDO model, while more complex to fit, much more closely resembles the data presented. Regions above and below the peak, at approximately 3.5 GHz, are matched well. Bicknell et al. raised concerns about the validity of their model given that it was based on several small sets of data points. These concerns are ameliorated by the the availability of 38 homogenous flux measurements for this source.

The predictive ability of the BDO model outside the range of the fit data was tested using two lower and one higher frequency data points. Table 3 shows these data and the corresponding BDO model predictions, with the results plotted in figure 2. The model cannot be directly evaluated at 403 MHz because the γ function is undefined, however, the model can be extended by treating the γ function as unity in this range. The model predictions for the 408 and 843 MHz frequencies fall slightly below the measured values. While the predicted values are lower than expected, the small number of low frequency data do not

Table 3. PKS 1718-649 low and high frequency data points

ν (GHz)	Flux (Jy)	BDO model (Jy)	Source
0.403	2.57 ± 0.12	3.22	Large and Cram (1995)
0.843	3.30	3.22	Molonglo Observatory Synthesis Telescope, Tingay et al. (1997)
22.2	1.75	2.36	Tidbinbilla 70m DSN Telescope, Tingay et al. (1997)
90	0.73	1.02	Swedish-ESO Submillimetre Telescope (SEST), Tingay et al. (1997)

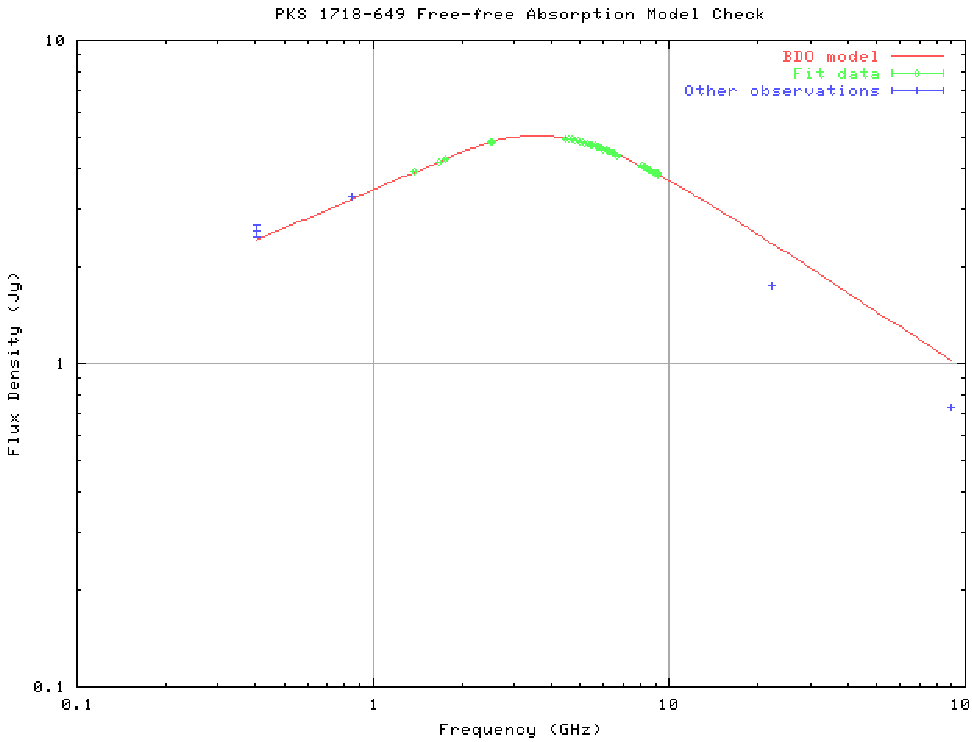

Fig. 2.— BDO model with third party data points

completely discredit the model. For the high frequency data the BDO model substantially over-estimates the flux density. Whether this is a substantial flaw in the model, the result of localised absorption features around 22 GHz and 90 GHz, measurement differences, or some other factor is not clear. Further high frequency samples, of comparable tenacity, in this region would be required to determine this.

The synthesised beam-width of the ATCA in the lowest frequency band is 6″, and in the highest band it is 1″. Therefore, the PKS 1718-649 source is not completely resolved by the ATCA in any of the observing bands and the measured signal is a composite of the two independent sources, identified by the SHEVE instrument, viewed from different directions. The effect of the composite nature is difficult to quantify but it may have a confusing effect on the model leading to the discrepancies with third-party data. Further, potentially wide beam-widths for the sub-GHz measurements may have the effect of collecting more "stray" signal from surrounding regions leading to higher than expected flux. Conversely, at the high frequency end with narrower beam-widths the measurement may underestimate the "true" figure. Such effects would be consistent with the low and high frequency observation vs. model differences.. A series of equal-beam-width measurements across the entire frequency band should remove this issue.

5. Conclusions

The simple model of a uniform free-free absorption screen imposed on a synchrotron source does not adequately describe the PKS 1718-649 data. While a reasonable match at frequencies above the peak, the model fails badly below the peak.

The ability of the BDO model to closely match these high precision measurements of PKS 1718-649 lends weight to the FFA model in general. There is clearly some degree of validity in the model within the peak region. In frequency regions above and below the ATCA samples the model over and underestimates, respectively, the flux density measurements from other sources. The paucity of data in these regions needs to be addressed to provide a better outline of the spectrum and exclude localised or instrumental effects as the cause of the discrepancies.

The BDO model does not conclusively exclude SSA as either a main or contributing factor in the emission peak. Similar high precision data for other sources could help to generalise this support. Mutoh et al. (2002) suggest that analysis of polarisation changes around the peak of a GPS source can be used to distinguish SSA from FFA. If this is indeed the case then the source of the peak may be settled.

The Australia Telescope is funded by the Commonwealth of Australia for operation as a national facility managed by the CSIRO.

REFERENCES

G. V. Bicknell, M. A. Dopita, and C. P. O. O'Dea. Unification of the Radio and Optical Properties of Gigahertz Peak Spectrum and Compact Steep-Spectrum Radio Sources. *ApJ*, 485:112–+, August 1997.

R. A. E. Fosbury, U. Mebold, W. M. Goss, and H. van Woerden. A radio and optical study of the galaxy PKS 1718-649. *MNRAS*, 179:89–97, April 1977.

Z. Kuncic, G. V. Bicknell, and M. A. Dopita. Induced Compton Scattering in Gigahertz Peak Spectrum Radio Sources. *ApJ*, 495:L35+, March 1998.

M. I. Large and L. E. Cram. Molonglo Reference Catalogue of Radio Sources (Large+ 1991). *VizieR Online Data Catalog*, 8016:0–+, August 1995. PKS 1718-649, 408Mhz, 2.57+/-0.12 Jy.

M. Mutoh, M. Inoue, S. Kameno, K. Asada, F. Kenta, and Y. Uchida. A New Test for the

Absorption Mechanism of GPS Radio Sources Using Polarization Properties. *PASJ*, 54:131–138, February 2002.

C. P. O'Dea. The Compact Steep-Spectrum and Gigahertz Peaked-Spectrum Radio Sources. *PASP*, 110:493–532, May 1998.

R. A. Preston, D. L. Jauncey, D. L. Meier, A. K. Tzioumis, J. Ables, R. Batchelor, J. Faulkner, J. Gates, B. Greene, P. A. Hamilton, B. R. Harvey, R. F. Haynes, B. Johnson, K. Lambeck, A. P. Louie, P. McCulloch, G. Moorey, D. D. Morabito, G. D. Nicolson, A. E. Niell, J. G. Robertson, G. R. Royle, L. Skjerve, M. A. Slade, O. B. Slee, A. Stolz, A. Watkinson, A. E. Wehrle, and A. E. Wright. The Southern Hemisphere VLBI experiment. *AJ*, 98:1–26, July 1989.

S. J. Tingay and M. de Kool. Radio spectral variability of the nearby GPS galaxy PKS 1718-649. *Publications of the Australian Astronomical Society*, in press, 2002.

S. J. Tingay, D. L. Jauncey, J. E. Reynolds, A. K. Tzioumis, E. A. King, R. A. Preston, J. E. J. Lovell, P. M. McCulloch, M. E. Costa, G. Nicolson, A. Koekemoer, M. Tornikoski, L. Kedziora-Chudczer, and D. Campbell-Wilson. The Nearest GHz Peaked-Spectrum Radio Galaxy, PKS 1718-649. *AJ*, 113:2025–2030, June 1997.

S. J. Tingay and D. W. Murphy. Estimates of the Free-Free Optical Depth toward the Subparsec-Scale Radio Source in Centaurus A. *ApJ*, 546:210–215, January 2001.

This preprint was prepared with the AAS LaTeX macros v5.0.